

Stable spatiotemporal solitons in Bessel optical lattices

D. Mihalache^{1,2,3}, D. Mazilu^{1,3}, F. Lederer¹, B. A. Malomed⁴,

Y. V. Kartashov², L.-C. Crasovan^{2,3}, and L. Torner²

¹ *Institute of Solid State Theory and Theoretical Optics,*

Friedrich-Schiller Universität Jena, Max-Wien-Platz 1, D-07774 Jena, Germany

²*ICFO-Institut de Ciencies Fotoniques,*

and Department of Signal Theory and Communications,

Universitat Politecnica de Catalunya, 08034 Barcelona, Spain

³*Department of Theoretical Physics, Institute of Atomic Physics,*

P.O. Box MG-6, Bucharest, Romania

⁴*Department of Interdisciplinary Studies, Faculty of Engineering,*

Tel Aviv University, Tel Aviv 69978, Israel

Abstract

We investigate the existence and stability of three-dimensional (3D) solitons supported by cylindrical Bessel lattices (BLs) in self-focusing media. If the lattice strength exceeds a threshold value, we show numerically, and using the variational approximation, that the solitons are stable within one or *two* intervals of values of their norm. In the latter case, the Hamiltonian-vs.-norm diagram has a “swallowtail” shape, with three cuspidal points. The model applies to Bose-Einstein condensates (BECs) and to optical media with saturable nonlinearity, suggesting new ways of making stable 3D BEC solitons and “light bullets” of an arbitrary size.

PACS numbers: 42.65.Tg, 42.65.Jx

Nonlinear wave dynamics in lattice potentials has well-known realizations in a wide range of physical settings, such as localized modes in solid-state lattices [1] and waves in Bose-Einstein condensates (BECs) trapped in optical lattices (OLs) [2]. Important realizations were predicted in optics, in terms of the light transmission in arrays of coupled nonlinear waveguides [3] and optically-induced structures in photorefractive (PR) materials (see surveys of recent results in Refs. [4] and [5]), in layered slab media [6], etc. Stable solitary pulses trapped in lattices in dissipative media were also predicted [7]. Experiments demonstrate that lattices in PR crystals indeed give rise to localized quasi-discrete dynamical patterns, such as fundamental spatial solitons [8], vortices [9], and soliton trains [10].

Optical spatiotemporal solitons (alias “light bullets”) have attracted a lot of attention in the last several years, see a review [11]. They are 3D wave packets in which the dispersion and diffraction are simultaneously balanced by nonlinearity. The search for suitable media for the creation of stable “bullets” is a challenging problem, as multidimensional solitons in Kerr-type focusing media are unstable against collapse (blowup) [12]. The same problem impedes creation of multidimensional solitons in self-attractive BECs. Various schemes to stabilize solitons in cubic media were proposed. In terms of BECs, a promising avenue is the use of periodic OL potentials. 2D and 3D solitons can be stabilized by OLs having the same dimension [13], or by *low-dimensional* OLs, i.e., 2D and 3D solitons may be stable in the presence of a 1D and 2D lattice, respectively [14, 15]; a 1D lattice can support stable 3D solitons in combination with the time-periodic alteration of the nonlinearity sign, provided by the Feshbach resonance [16]. An essential advantage offered by the low-dimensional OLs is that the solitons can freely move in the unconfined direction(s), which opens a way to study their collisions and bound states [14, 16]. Essentially new possibilities are opened in optics and BECs by radial OLs with axial symmetry, that can be induced by diffraction-free cylindrical Bessel beams [17]. Several 2D soliton families, including fundamental solitons trapped at the center or in different rings of the Bessel lattice (BL) and dipole-mode solitons, were predicted in a cubic nonlinear medium, and were shown to be stable in certain parameter domains [18]. Very recently, stable ring-shaped solitons in cylindrical lattices were also predicted in media with the saturable nonlinearity of the PR type [19].

The difference between the previously studied 2D periodic OLs and the BL is more than just another symmetry. First, the BL makes it possible to create a soliton at a prescribed location (if the experimental field is large enough, several solitons can be created and ma-

nipulated simultaneously). Moreover, each soliton can be moved across the field by a slowly sliding laser beam. Soliton networks and wires can be also created with arrays of Bessel beams, a goal hard to achieve with harmonic lattices. Quite important is also the difference in the spatial scales. Indeed, the period of OLs is dictated by the laser-beam's wavelength, λ_0 (although the period can be made larger by launching the interfering waves under an angle to each other [5]). On the contrary, the radial scale of the BL is completely independent of λ_0 , being determined by the phase mask through which the beam is passed. The use of the BL with an essentially large scale will make it possible to create big *paraxial solitons* in optical media, and big solitons in BEC. The scale difference also highlights the distinction of the BL from the single-mode optical fibers, or cigar-shaped traps in BEC [20], where the radius is also limited to microns.

The subject of this work are 3D solitons trapped in the BL, in the case of the cubic self-attraction. This configuration can be directly implemented in BECs with a negative scattering length, illuminated by an optical Bessel beam. The corresponding normalized 3D Gross-Pitaevskii equation (GPE) for the wave function q is [2]

$$i\frac{\partial q}{\partial \xi} = -\frac{1}{2}\left(\frac{\partial^2 q}{\partial \eta^2} + \frac{\partial^2 q}{\partial \zeta^2} + \frac{\partial^2 q}{\partial \tau^2}\right) - |q|^2 q - \Pi(r)q, \quad (1)$$

where ξ is time, τ and (η, ζ) are, respectively, the coordinates along the beam and in the transverse plane, $r \equiv (\eta^2 + \zeta^2)^{1/2}$, and the potential function $\Pi(r)$ is proportional to the local intensity of the red-detuned optical wave which traps atoms at its anti-nodes [2] [being interested in self-supporting solitons, we do not include a magnetic (parabolic) trapping potential]. In this work we mainly concentrate on the case of $\Pi(r) = pJ_0(\sqrt{2\beta}r)$, with the Bessel function J_0 generated by the diffraction-free cylindrical beam [17]. Constants p and β determine the strength and radial scale of the BL. Note that the effective potential created by the Bessel beam proper is proportional to $-J_0^2$, while the case of $\Pi \sim J_0$ actually implies interference between the cylindrical beam and a stronger plane wave with an amplitude A_0 at the same frequency. Indeed, the latter configuration implies the full field amplitude $A(r) = A_0 + A_1 e^{i\chi} J_0(\sqrt{2\beta}r)$ (with constant A_1 and a phase shift χ), which generates the above potential through the expansion $|A(r)|^2 \approx A_0^2 + 2A_0 A_1 (\cos \chi) J_0(\sqrt{2\beta}r)$. We demonstrate below that the 3D solitons supported by the potentials $-J_0^2$ and $-J_0$ may differ because of different degrees of localization of these potentials. The latter potential (which was not proposed before) may be more convenient, as it may be controlled by the phase

shift χ ; in particular, it is possible to flip the sign of the J_0 potential, which is impossible for its J_0^2 counterpart.

In nonlinear optics, ξ , (η, ζ) , and τ are, respectively, normalized propagation and transverse coordinates and local time [11], assuming anomalous chromatic dispersion. Then, Eq. (1) governs the nonlinear transmission of a probe signal in a strong BL induced by a pump beam launched in an orthogonal polarization, or at a different wavelength. In this case, $\Pi(r)$ measures local modulation of the refractive index for the probe signal induced by the pump beam through the cross-phase modulation, and the choice of $\Pi \sim J_0$ again implies the interference between the Bessel beam and a stronger plane wave. The pump beam is assumed to propagate in a nearly linear regime, that actually implies strong saturation of the pump beam in the medium with saturable nonlinearity.

Equation (1) conserves the norm, $U = \int \int \int |q(\eta, \zeta, \tau)|^2 d\eta d\zeta d\tau$, Hamiltonian, H , and angular momentum. We search for stationary solitons, $q(\eta, \zeta, \tau, \xi) = w(r, \tau) \exp(ib\xi)$, where b is a real propagation constant, and w , which must vanish at $|\tau|, r \rightarrow \infty$, obeys the equation

$$w_{\tau\tau} + w_{rr} + r^{-1}w_r + 2[p\Pi(r) - b]w + 2w^3 = 0. \quad (2)$$

In numerical calculations, we fix the radial scale, $\beta \equiv 10$, and vary b and p (cf. Ref. [18]).

Using an obvious Lagrangian representation of Eq. (2), we start with the variational approximation (VA). To this end, we adopt the Gaussian *ansatz* for the 3D soliton, $w(r, \tau) = A \exp[-(\tau^2/T^2 + r^2/R^2)/2]$, with free parameters T , R and A . The known procedure [21] leads to relations $T^2 = R^2 / (1 - p\beta R^4 e^{-\beta R^2/2})$, $b = p(1 - 3\beta R^2/4) e^{-\beta R^2/2} + (4R^2)^{-1}$, and $U^2 = 8\pi^3 R^2 (1 - p\beta R^4 e^{-\beta R^2/2})$, where $U = \pi^{3/2} A^2 T R^2$ is the soliton's norm. These equations predict the main characteristic of the soliton family, $U(b)$. Then, the Vakhitov-Kolokolov (VK) criterion, $dU/db > 0$, provides for stability of the solitons against perturbations with real eigenvalues [12]. A first VK-stable interval appears around $R = R_0^{(1)} \equiv 2.75/\sqrt{\beta}$, when the BL strength attains a threshold value, $p_{\text{thr}}^{(1)} \approx 0.12\beta$. A *second stability interval* appears around $R_0^{(2)} \equiv [2(3 - \sqrt{3})/\beta]^{1/2} \approx 1.59/\sqrt{\beta}$, when p passes a *second threshold*, $p_{\text{thr}}^{(2)} \approx 0.32\beta$. As shown below, numerical results confirm the existence of two stability intervals for $p > p_{\text{thr}}^{(2)}$. It is relevant to compare the above values $R_0^{(1,2)}$ and the size of the central core of the BL potential in Eq. (2), which is determined by the first zero of the function $J_0(\sqrt{2\beta}r)$, $r_0 \approx 1.70/\sqrt{\beta}$. The comparison suggests that the above simple *ansatz*, that neglects BL-induced fringes in the shape of the soliton, is appropriate, as the

predicted solitons do not cover many rings of the radial lattice.

Numerically, soliton families were found from Eqs. (2) by means of the relaxation method. Simulations of the full GPE (1) were carried out using the Crank-Nicholson scheme. To test the stability, we took perturbed solutions as $q = [w(r, \tau) + u(r, \tau) \exp(\delta\xi + in\phi) + v^*(r, \tau) \exp(\delta^*\xi - in\phi)] \exp(ib\xi)$, where ϕ is the azimuthal angle in the plane (η, ζ) , and $n = 0, 1, 2, \dots$. The linearization of Eq. (1) leads to straightforward equations for the perturbation mode (u, v) and its growth rate δ . The numerical results are summarized in Fig. 1. We found that the 3D solitons exist in the J_0 potential if the propagation constant b exceeds a certain cutoff value b_{co} . Figure 1(a) shows that b_{co} increases with the BL strength p [$b_{co}(p)$ vanishes at $p = 0$ as unstable free-space 3D solitons exist for all $b > 0$]. The soliton's norm U is a *non-monotonous* function of b , see Fig. 1(b). The prediction of the VK criterion, that parts of the soliton family with $dU/db > 0$ may be stable, was verified by numerical computation of the growth rates, $\text{Re}(\delta)$. It was found that the solitons are completely stable *precisely* in regions singled out by the condition $dU/db > 0$, see Fig. 1(c). For the J_0 potential and relatively small values of the BL strength p , the solitons are stable in a narrow interval of b to the right of b_{co} [see a small solid segment of the curve in Fig. 1(b) corresponding to $p = 5$]. Losing their stability for b exceeding the value at which dU/db vanishes, the 3D solitons drastically differ from their BL-supported 2D counterparts, that may be stable in their entire existence domain if the lattice strength p is large enough [18]. Remarkably, for moderate values of p , the 3D solitons are stable in *two disjoint intervals* of b [one abuts on the cutoff point, $b = b_{co}$, and the other is found at relatively large values of b , see the curve corresponding to $p = 5.5$ in Fig. 1(b)]. This feature was predicted above by the VA. However, there is *only one* soliton-stability domain, adjacent to the cutoff, for the J_0^2 potential, see Fig. 1(d). The difference can be traced to different localization degrees of the J_0^2 and J_0 potentials.

The Hamiltonian-vs.-norm diagrams for the soliton families, which is a useful tool for the analysis of the soliton stability [22], are plotted in Fig. 2. With the J_0 potential, they exhibit one or three cuspidal points. In the latter case [Fig. 2(a)], the diagram features a “swallowtail” pattern, which accounts for the existence of the two above-mentioned distinct stability regions for the 3D solitons. Although this pattern is one of generic possibilities known in the catastrophe theory, it rarely occurs in physical models [22]. In Fig. 3 we display three typical examples of stable 3D solitons supported by the J_0 potential. A low-

amplitude broad soliton covering several lattice rings, with the propagation constant b close to the cutoff b_{co} , is shown in Fig. 3(a), and high-amplitude narrow solitons, mostly trapped within the BL core, are presented in Figs. 3(b,c).

An important issue for the 3D solitons in the focusing medium is the occurrence of collapse. We expect that the solitons which are unstable against small perturbations either undergo the collapse, or decay into radiation waves, depending on the perturbation. To test these expectations, we simulated the evolution of perturbed solitons, starting with $q(\xi = 0) = w(\eta, \zeta, \tau)(1 + \epsilon f)$, where ϵ is a small perturbation amplitude, and f is either a random variable uniformly distributed in the interval $[-1, 1]$, or constant, $f = 1$. We have found that the solitons which were predicted to be stable in terms of the perturbation eigenvalues are indeed stable in the direct simulations. As an example, in Fig. 4 we show the evolution of a soliton with a random perturbation whose amplitude is $\epsilon = 0.05$. Despite a considerable transient change of its shape, the soliton relaxes to a self-cleaned form which is quite close to the unperturbed one. Under the same random perturbation, linearly unstable solitons were found to decay into radiation. The uniform initial perturbation, $f = 1$, amounts to an instantaneous change of the soliton's amplitude. This perturbation excites persistent oscillations of linearly stable solitons, while the effect on linearly unstable ones is completely different from the response to random perturbations: they do not decay, but, instead, blow up.

In conclusion, we have constructed families of 3D solitons supported by zero-th order Bessel optical lattices. We have found that, in one or *two* intervals, the solitons are stable, provided that the lattice is strong enough. We also expect that 3D solitons can be stabilized by higher-order Bessel lattices, too. This is the first example of a 3D soliton stabilized by an axially symmetric lattice; unlike stable 3D solitons in 2D periodic lattices, the soliton's size is not determined by the wavelength of the laser beam, but may be chosen at will. Depending on the lattice strength, the Hamiltonian-vs.-norm diagram for solitons in the J_0 potential displays a “swallowtail” bifurcation, a rare phenomenon in physics.

The results suggest new approaches to the still unresolved [11] problem of the creation of 3D solitons in the experiment. One possibility is to make a BEC soliton in the cylindrical optical lattice, which may be controlled by the superposition of the Bessel beam and uniform background field. In optics, creation of the 3D lattice solitons require the bimodal setting in a medium with saturable nonlinearity. In all these settings, stable 3D solitons are predicted

to feature universal properties.

Support from Deutsche Forschungsgemeinschaft (DFG), Institució Catalana de Recerca i Estudis Avançats (ICREA), and the Israel Science Foundation (grant No. 8006/03) is acknowledged.

-
- [1] W.P. Su, J.R. Schrieffer, and A.J. Heeger, Phys. Rev. Lett. **42**, 1698 (1979); A.J. Sievers and S. Takeno, *ibid.*, **61**, 970 (1988); M. Sato and A.J. Sievers, Nature **432**, 486 (2004).
 - [2] B.P. Anderson and M. Kasevich, Science **282**, 1686 (1998); A. Trombettoni and A. Smerzi, Phys. Rev. Lett. **86**, 2353 (2001); F.S. Cataliotti *et al.*, Science **293**, 843 (2001); M. Greiner *et al.*, Phys. Rev. Lett. **87**, 160405 (2001); Nature **415**, 39 (2002).
 - [3] D.N. Christodoulides and R.I. Joseph, Opt. Lett. **13**, 794 (1988).
 - [4] D.N. Christodoulides, F. Lederer, and Y. Silberberg, Nature **424**, 817 (2003).
 - [5] J.W. Fleischer *et al.*, Opt. Exp. **13**, 1780 (2005).
 - [6] B.A. Malomed *et al.*, J. Opt. Soc. Am. B **16**, 1197 (1999); W.D. Li and A. Smerzi, Phys. Rev. E **70**, 016605 (2004); I.M. Merhasin *et al.*, *ibid.* **71**, 016613 (2005).
 - [7] K. Staliunas, Phys. Rev. Lett. **91**, 053901 (2003).
 - [8] J.W. Fleischer *et al.*, Nature **422**, 147 (2003); Phys. Rev. Lett. **90**, 023902 (2003); D. Neshev *et al.*, Opt. Lett. **28**, 710 (2003).
 - [9] D. Neshev *et al.*, Phys. Rev. Lett. **92**, 123903 (2004); J.W. Fleischer *et al.*, *ibid.* **92**, 123904 (2004).
 - [10] Z. Chen *et al.*, Phys. Rev. Lett. **92**, 143902 (2004); Y.V. Kartashov *et al.*, Opt. Express **12**, 2831 (2004).
 - [11] B.A. Malomed, D. Mihalache, F. Wise, and L. Torner, J. Opt. B: Quantum Semiclass. Opt. **7**, R53 (2005).
 - [12] L. Bergé, Phys. Rep. **303**, 260 (1998).
 - [13] B.B. Baizakov, B.A. Malomed, and M. Salerno, Europhys. Lett. **63**, 642 (2003); Z.H. Musslimani and J. Yang, J. Opt. Soc. Am. B **21**, 973 (2004); Y.V. Kartashov *et al.*, Opt. Lett. **29**, 1918 (2004).
 - [14] B.B. Baizakov, B.A. Malomed, and M. Salerno, Phys. Rev. A **70**, 053613 (2004).
 - [15] D. Mihalache *et al.*, Phys. Rev. E **70**, 055603(R) (2004).

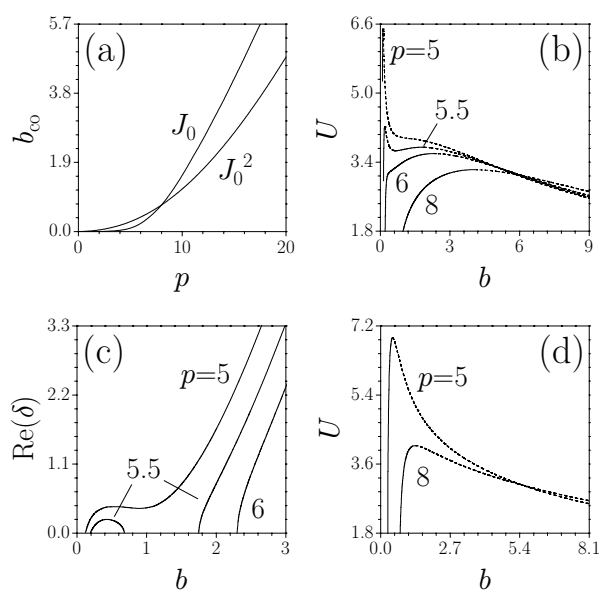
- [16] M. Trippenbach, M. Matuszewski, and B.A. Malomed, *Europhys. Lett.* **70**, 8 (2005).
- [17] J. Durnin, J.J. Miceli, and J.H. Eberly, *Phys. Rev. Lett.* **58**, 1499 (1987).
- [18] Y.V. Kartashov, V.A. Vysloukh, and L. Torner, *Phys. Rev. Lett.* **93**, 093904 (2004); **94**, 043902 (2005).
- [19] Q.E. Hoq *et al.*, *Phys. Lett. A*, in press.
- [20] K.E. Strecker *et al.*, *Nature* **417**, 153 (2002); L. Khaykovich *et al.*, *Science* **296**, 1290 (2002).
- [21] B.A. Malomed, *Progr. Optics* **43**, 71 (2002).
- [22] F.V. Kusmartsev, *Phys. Rep.* **183**, 1 (1989).

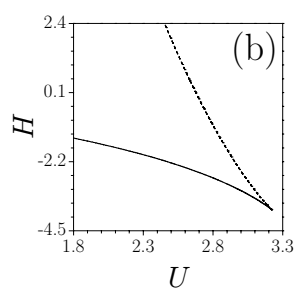
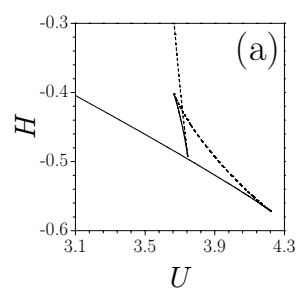
FIG. 1: (a) The propagation constant cutoff vs. the lattice strength, shown for the cylindrical potentials of both types, J_0 and J_0^2 . (b,d) The soliton's norm vs. the propagation constant for the potentials J_0 and J_0^2 , respectively. (c) The perturbation growth rate vs. the propagation constant for the J_0 potential. Here and below, solid and dashed curves correspond, respectively, to stable and unstable branches.

FIG. 2: The Hamiltonian-vs.-norm diagrams for $p = 5.5$ (a) and 8 (b). Here and below, all the figures are shown for the J_0 potential.

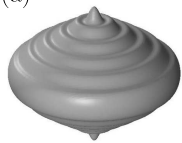
FIG. 4: The evolution of a stable soliton under a random perturbation, for $p = 5$, $b = 0.11$, $U = 6.477$: (a) $\xi = 0$, (b) $\xi = 200$, (c) $\xi = 500$.

FIG. 3: Isosurface plots for stable solitons: (a) $p = 5$, $b = 0.11$, $U = 6.477$; (b) $p = 5.5$, $b = 0.85$, $U = 3.677$; (c) $p = 6$, $b = 2$, $U = 3.591$.

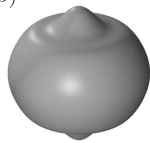




(a)



(b)



(c)

